

See discussions, stats, and author profiles for this publication at: <https://www.researchgate.net/publication/261440255>

# Investigation on the structural stability and electronic properties of InSb nanostructures – A DFT approach

ARTICLE *in* AEJ - ALEXANDRIA ENGINEERING JOURNAL · JUNE 2014

DOI: 10.1016/j.aej.2014.03.008

---

CITATIONS

13

---

READS

42

2 AUTHORS, INCLUDING:



[R. Chandiramouli](#)

SASTRA University

67 PUBLICATIONS 300 CITATIONS

SEE PROFILE



Alexandria University  
**Alexandria Engineering Journal**

[www.elsevier.com/locate/aej](http://www.elsevier.com/locate/aej)  
[www.sciencedirect.com](http://www.sciencedirect.com)



ORIGINAL ARTICLE

# Investigation on the structural stability and electronic properties of InSb nanostructures – A DFT approach



V. Nagarajan, R. Chandiramouli \*

*School of Electrical & Electronics Engineering, SASTRA University, Tirumalaisamudram, Thanjavur 613 401, India*

Received 9 November 2013; revised 3 March 2014; accepted 13 March 2014

Available online 8 April 2014

## KEYWORDS

Nanostructures;  
Indium antimonide;  
Binding energy;  
Embedding energy;  
Electronic property

**Abstract** The realistic InSb nanostructures namely InSb nanoring, InSb nanocube, InSb nanocube-18, InSb nanosheet, InSb nanocage and InSb nanocube-27 are simulated and optimized successfully using B3LYP/LanL2DZ basis set. The stability of InSb nanostructures is studied in terms of binding energy, vibrational studies and calculated energy. The electronic properties of InSb nanostructures are discussed using ionization potential, electron affinity and HOMO–LUMO gap. Point symmetry and dipole moment of InSb nanostructures are reported. Incorporation of impurity atom in InSb nanostructures is studied using embedding energy. The present study provides the information regarding the enhanced electronic properties of InSb nanostructure which finds its potential importance in microelectronics and optoelectronic devices.

© 2014 Production and hosting by Elsevier B.V. on behalf of Faculty of Engineering, Alexandria University.

## 1. Introduction

Indium antimonide (InSb), indium phosphide (InP) and gallium arsenide (GaAs) are most important materials in both microelectronics and optoelectronics industries [1]. Particularly InSb has maximum drift velocity and high value of elec-

tron mobility. InSb detectors have sensitivity range from 1–5  $\mu\text{m}$  wavelengths. InSb is a narrow gap semiconductor material and belongs to III–V group compound semiconductor used in thermal imaging camera; it is best choice to fabricate photoconductors, magnetoresistors and infrared detectors [2].

The electronic properties of semiconductor mainly depend on defects, dopants and contaminants [3]. These parameters should be managed critically so that the semiconductor properties can be controlled precisely. The determination of dopants as well as defects is very important to tailor a functional material. Shiue et al. reported determination of tellurium in indium antimonide semiconductor material by electrothermal atomic absorption spectrometry [4]. Fulop et al. synthesized polycrystalline InSb from aqueous electrolytes by using electrodeposition method [5]. Sun et al. studied the effect of antimony in the growth of indium arsenide quantum dots in

\* Corresponding author. Tel.: +91 9489566466; fax: +91 4362 264120.

E-mail address: [rcmouli@gmail.com](mailto:rcmouli@gmail.com) (R. Chandiramouli).

Peer review under responsibility of Faculty of Engineering, Alexandria University.



Production and hosting by Elsevier

**Nomenclature**

InSb	indium antimonide	DOS	density of states
DFT	density functional theory	EA	electron affinity
NWChem	high-performance computational chemistry software	IP	ionization potential
B3LYP	Becke, three-parameter, Lee–Yang–Parr (exchange–correlation energy functional)	BE	binding energy
LanL2DZ	Los Alamos National Laboratory 2-double zeta basis set	EE	embedding energy
DM	dipole moment	IR intensity	infra-red intensity
HOMO	highest occupied molecular orbital	$E(\text{In})$	energy of indium atom
LUMO	lowest unoccupied molecular orbital	$E(\text{Sb})$	energy of antimony atom
		$E(\text{InSb})$	energy of indium antimonide nanostructure
		$n$	total number of atoms in nanostructure

gallium arsenide (001) [6]. Seol et al. reported measurement of thermopower and electrical conductivity of indium antimonide nanowire from a vapor–liquid–solid method [7].

The objective of the present work is to identify the appropriate nanostructure of InSb which leads to enhanced structural stability and electronic properties of InSb nanostructures. Based on these aspects the literature survey was conducted and most of the reported work mainly deals with synthesis of InSb and characterization of InSb. Density functional theory (DFT) is a suitable method to fine-tune electronic properties of nanostructures [8]. In the present work different structure of InSb nanostructures is optimized and simulated successfully by using DFT and the results are reported.

## 2. Computational details

The nanostructures of InSb are successfully optimized using NWChem package [9]. Indium has the atomic number of forty-nine and atomic number of antimony is fifty-one. LanL2DZ basis set is good choice to optimize InSb nanostructures along with Becke's three-parameter hybrid function (B3LYP) [10–14]. Moreover LanL2DZ basis set can be applied to the following elements such as H, Li–La and Hf–Bi. These elements provide the optimum output with the pseudo potential approximation [15]. Density functional theory (DFT) is better choice to compute stability and electronic properties of nanoclusters which depend on electron density functional and it is suitable to study InSb nanostructures. Six different InSb nanostructures are constructed and simulated successfully and the results are reported.

## 3. Results and discussion

The present work mainly focuses on HOMO–LUMO gap, calculated energy, electron affinity (EA), ionization potential (IP), dipole moment (DM), binding energy (BE), embedding energy (EE) and vibrational studies of InSb nanostructures. Six different InSb nanostructures are named as InSb nanocube-27, InSb nanocube-18, InSb nanocube, InSb nanosheet, InSb nanoring and InSb nanocage. InSb nanostructures are shown in Fig. 1(a)–(f). InSb nanocube-27 has fourteen antimony atoms and thirteen indium atoms and it resembles a three dimensional cubic structure. Nine In atoms combined with

nine Sb atoms form InSb nanocube-18 structure, and InSb nanocube consists of eight In atoms and eight Sb atoms which resembles extended cube structure. InSb nanoring is formed by the combination of five In atoms and five Sb atoms to form a ring like structure. InSb nanosheet has twelve In atoms and twelve Sb atoms followed by InSb nanocage which has thirteen Sb atoms and thirteen In atoms to form cage like structure.

The stability of InSb nanostructures can be discussed in terms of calculated energy ( $E$ ) as shown in Table 1. The energy of InSb nanoring is found to be  $-35.952$  Hartrees. For InSb nanocube the energy is  $-55.391$  Hartrees and InSb nanocube-18 has  $-62.021$  Hartrees. InSb nanosheet, InSb nanocage and InSb nanocube-27 are calculated to be  $-83.880$  Hartrees,  $-90.518$  Hartrees and  $-94.059$  Hartrees, respectively. The stability of the nanostructure gradually increases with an increase in the number of atoms in nanostructure. Dipole moment (DM) found to be low for InSb nanoring, InSb nanocube and InSb nanocube-27 in the range of  $0.28$ – $0.68$  Debye, and it reveals the arrangement of atoms inside the nanostructure. The low value indicates that the atoms are well packed and charges present inside the nanostructures are uniformly distributed. In contrast, DM of InSb nanocage, InSb nanosheet and InSb nanocube-18 are high in the range from  $2.54$  to  $4.94$  Debye, due to improper distribution of charges in nanostructures. The point group of all the simulated nanostructures is  $C_1$  except for InSb nanoring which is  $C_5$ . These point groups refers to asymmetry in the structure.

### 3.1. HOMO–LUMO gap of InSb nanostructures

The electronic properties of InSb nanostructures are discussed in terms of lowest unoccupied molecular orbital (LUMO) and highest occupied molecular orbital (HOMO) [16,17]. The HOMO–LUMO gap for all InSb nanostructures has low value in the order  $0.47$ – $0.92$  eV, and it is inferred that the InSb nanostructures are having narrow gap. The low value of gap in InSb nanostructures requires less energy to move the electron from HOMO level to LUMO level. Moreover, the localization of charges is high in conduction band than in the valence band. The localization of charge is more near the Fermi level ( $E_F$ ) which implies that less energy is enough to move electron from HOMO level to LUMO level. The localization of charges in the nanostructures is visualized by density of states (DOS) spectrum as shown in Table 2.

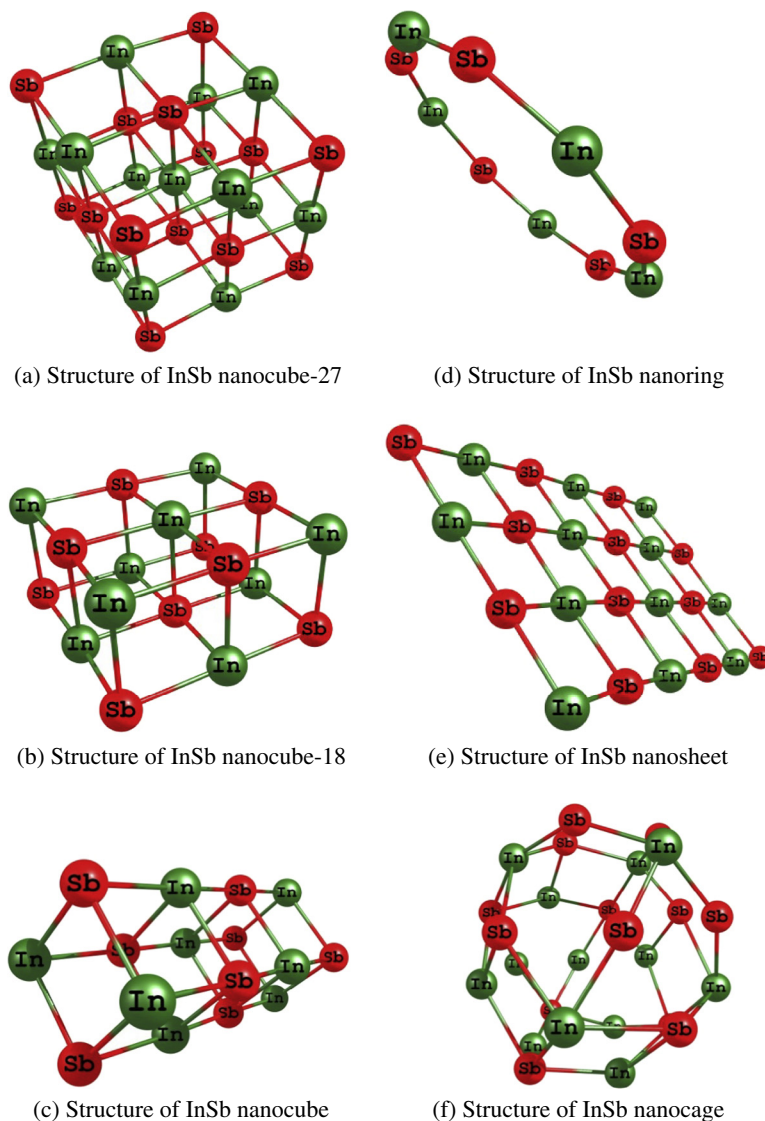


**Figure 1** InSb nanostructures.

**Table 1** Energy, dipole moment and point group of InSb nanostructures.

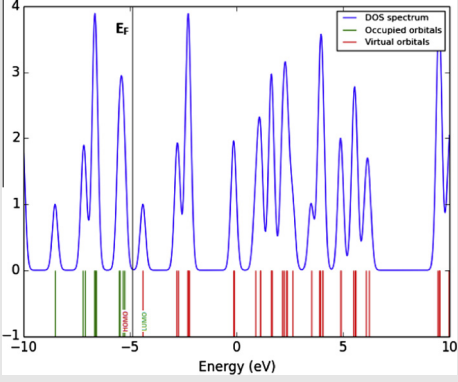
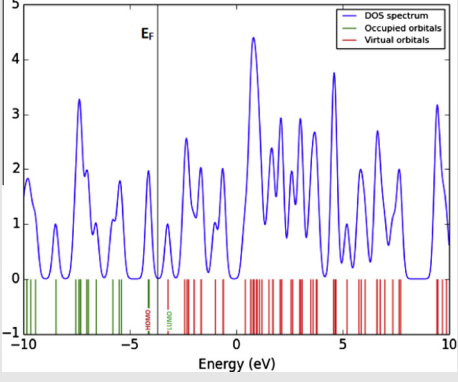
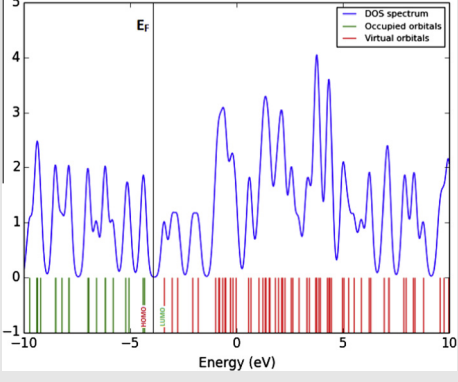
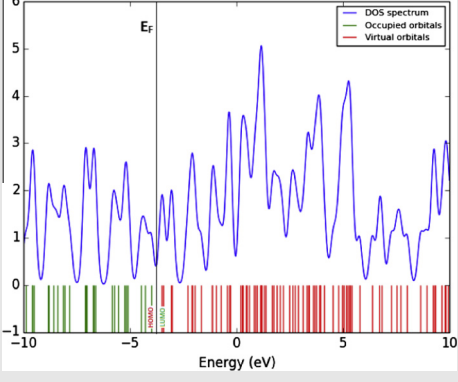
Structure	Energy (Hartrees)	DM (Debye)	Point group
InSb nanoring	-35.952	0.2806	C <sub>s</sub>
InSb nanocube	-55.391	0.5588	C <sub>1</sub>
InSb nanocube-18	-62.021	4.936	C <sub>1</sub>
InSb nanosheet	-83.880	3.1542	C <sub>1</sub>
InSb nanocage	-90.518	2.5397	C <sub>1</sub>
InSb nanocube-27	-94.059	0.6785	C <sub>1</sub>

### 3.2. Ionization potential and electron affinity of InSb nanostructures

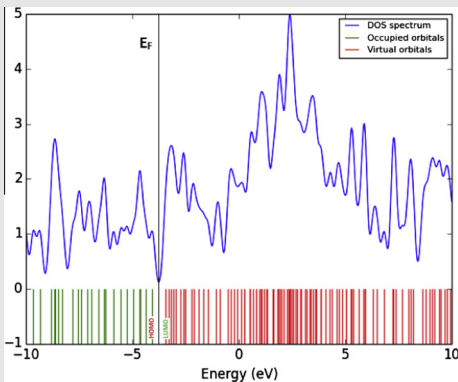
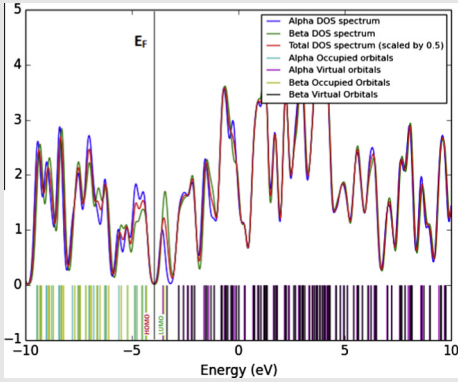
The electronic properties of InSb nanostructures can also be studied using electron affinity (EA) and ionization potential (IP). IP refers the energy released due to removing electron from the nanostructure and EA is the energy released due to

the addition of electron in the nanostructure [18–21]. EA plays a vital role in chemical sensors and also in plasma physics. Almost same trends are found in both IP and EA as shown in Fig. 2. In the case of InSb nanoring, IP and EA values are found to be high which is suitable for plasma physics and chemical sensors. However in the other structures due to the increase in the number of atoms, it leads to decrease the IP

**Table 2** HOMO, LUMO and DOS spectrum of InSb nanostructures.

Structure	HOMO	LUMO	$E_g$ (eV)	HOMO, LUMO and DOS spectrum
InSb nanoring	-5.27	-4.39	0.88	
InSb nanocube	-4.1	-3.22	0.88	
InSb nanocube-18	-4.32	-3.4	0.92	
InSb nanosheet	-4	-3.53	0.47	

(continued on next page)

Structure	HOMO	LUMO	$E_g$ (eV)	HOMO, LUMO and DOS spectrum
InSb nanocage	−4.05	−3.44	0.61	
InSb nanocube-27	−4.36	−3.57	0.79	

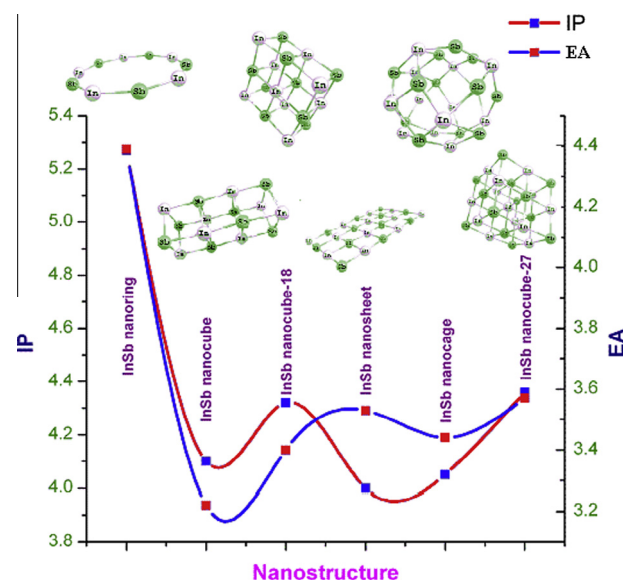


Figure 2 Ionization potential and electron affinity of InSb nanostructures.

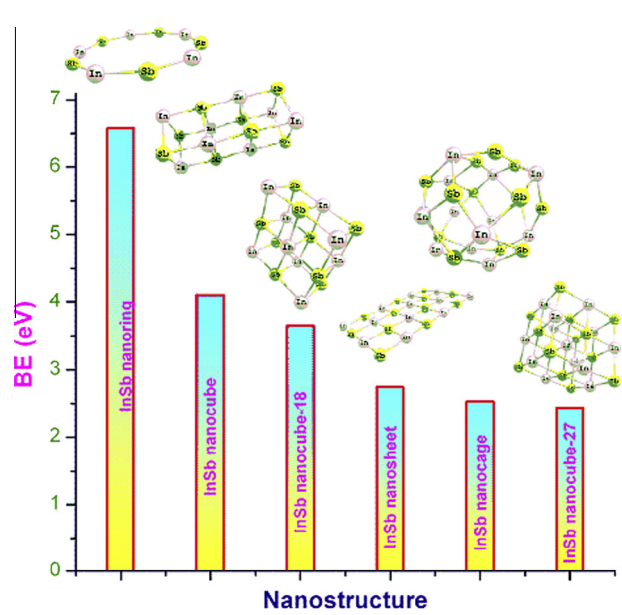
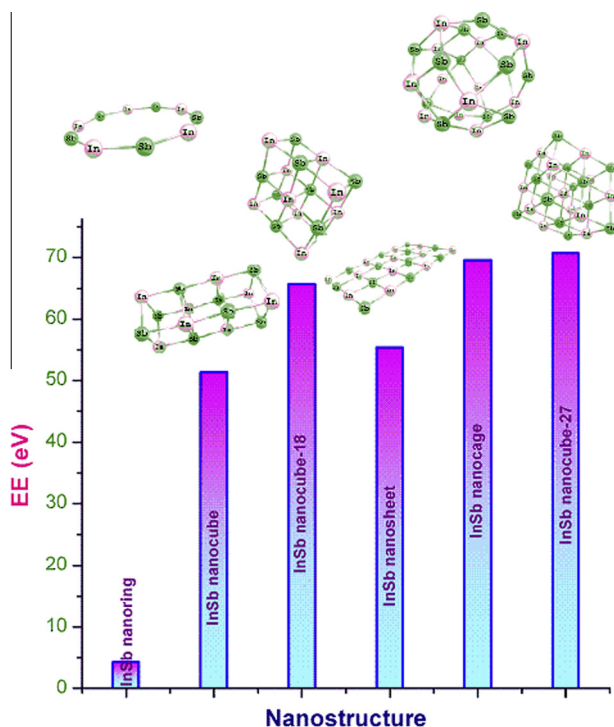


Figure 3 Nanostructures size vs binding energy.





**Figure 4** Nanostructures size vs embedding energy.

and EA. On observing all the structures nanocube and nanocage structures found to have low value of IP and EA which is not favorable structure for chemical sensors.

### 3.3. Binding energy and embedding energy of InSb nanostructures

The binding energy (BE) of InSb nanostructures can be calculated by the equation 1 as follows

$$BE = [(n^*E(\text{In}) + n^*E(\text{Sb}) - n^*E(\text{InSb}))]/n \quad (1)$$

where  $E(\text{In})$  is the energy of In atom,  $E(\text{Sb})$  is the energy of Sb atom and  $E(\text{InSb})$  is the energy of InSb nanostructure and  $n$  is the number of atoms in the nanostructure. BE also gives the precise data about the stability of the nanostructures [22–24]. InSb nanostructures are stable when the BE value is high. BE of InSb nanostructures increases with more number of atoms in nanostructure as shown in Fig. 3. InSb nanosheet, InSb nanocage and InSb nanocube-27 almost have same value of BE.

Embedding energy refers how far the substitution impurities can be incorporated in the nanostructure. The EE of InSb nanostructures is calculated using Eq. (2)

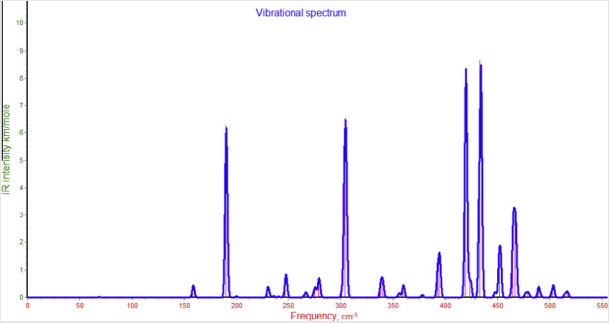
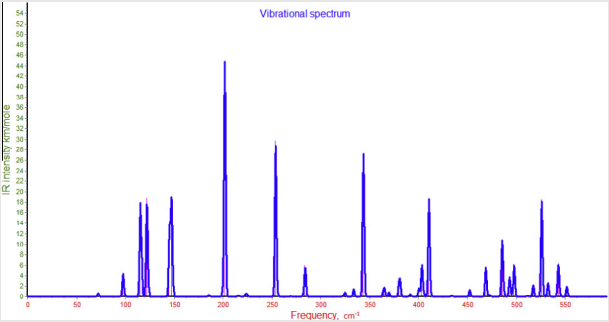
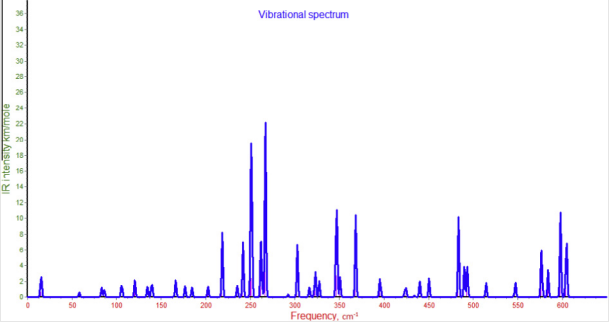
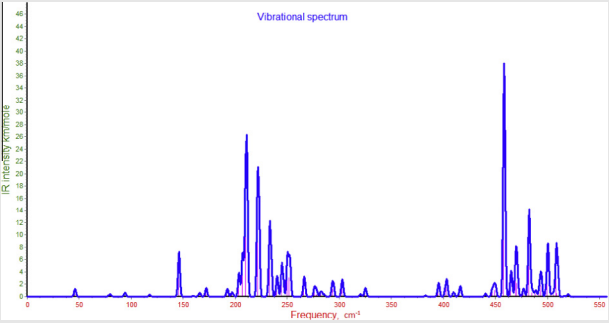
$$EE = [(n^*E(\text{In}) + n^*E(\text{Sb}) - n^*E(\text{InSb}))] \quad (2)$$

**Table 3** Vibrational frequency and IR intensity of InSb nanostructures.

	Vibrational frequency ( $\text{cm}^{-1}$ )	IR intensity ( $\text{km/mole}$ )	Mode assignment	IR spectrum
InSb nanoring	478.38 468.72	78.92 75.70	Molecular stretching	
InSb 2D nanocube	485.98 325.91	34.54 11.34	Molecular stretching	

(continued on next page)

Table 3 (continued)

	Vibrational frequency (cm <sup>-1</sup> )	IR intensity (km/mole)	Mode assignment	IR spectrum
InSb 3D nanocube-18	433.95 420.08	8.64 8.34	Molecular stretching	
InSb nanosheet	201.74 253.91	44.75 29.73	Molecular stretching	
InSb nanocage	266.92 250.71	5.86 3.90	Molecular stretching	
InSb 3D nanocube-27	458.49 210.59	19.23 13.16	Molecular stretching	

The EE is almost same for all the structures except for InSb nanoring. For all the nanostructures except for InSb nanoring, the EE ranges in the order of 51.28–70.57 eV. In contrast, the EE for InSb nanoring is

6.57 eV. It implies that tailoring the nanostructures in the form of nanoring will enhance the substitution of foreign atoms in the nanostructure. Fig. 4 depicts the EE of InSb nanostructures.



### 3.4. Vibrational studies of InSb nanostructures

The stability of the InSb nanostructure can also be defined by vibrational studies. The structure with no imaginary frequency is said to be more stable [25]. Vibrational frequencies and IR intensity of InSb nanostructures are tabulated in Table 3. InSb nanoring has the prominent vibrational frequency at 478.38 and 468.72  $\text{cm}^{-1}$  with IR intensity of 78.92 and 75.70 km/mole, respectively. In the case of InSb nanocube, vibrational frequency is observed at 485.98 and 325.91  $\text{cm}^{-1}$  which has the IR intensity of 34.54 and 11.34 km/mole, respectively. InSb nanocube-18 has the vibrational frequency of 433.95 and 420.08  $\text{cm}^{-1}$  with IR intensity observed at 8.64 and 8.34 km/mole. The prominent vibrational frequency of InSb nanosheet is observed at 201.74  $\text{cm}^{-1}$ , 253.91  $\text{cm}^{-1}$  with IR intensity of 44.75 km/mole and 29.73 km/mole, respectively. InSb nanocage has vibrational frequency at 266.92  $\text{cm}^{-1}$  with IR intensity of 5.86 km/mole and for frequency of 250.71  $\text{cm}^{-1}$  with intensity of 3.90 km/mole. InSb nanocube-27 has the vibrational frequency at 458.49 and 210.59  $\text{cm}^{-1}$  with IR intensity of 19.23 and 13.16 km/mole respectively.

### 4. Conclusion

In conclusion, InSb nanostructures are completely simulated and optimized using DFT with B3LYP/LanL2DZ basis set. Stability of InSb nanostructures is analyzed using binding energy, vibrational studies and calculated energy. Stability also depends on the number of atoms in nanostructure. The electronic properties are studied in terms of IP, EA and HOMO–LUMO gap. Point symmetry and dipole moment for different nanostructures of InSn are also reported. The embedding energy gives the details about the incorporation of foreign atoms in nanostructures. The information provided in the present work will give a clear picture to tailor InSb nanostructure with improved electronic properties in the microelectronics and optoelectronic devices.

### References

- [1] S.M. Sze, *Semiconductor Devices Physics and Technology*, Wiley, New York, 1985.
- [2] O. Sugiura, M. Matsumura, Homoepitaxial growth of InSb by vacuum metal-organic chemical vapor deposition, *J Appl Phys* 24 (1985) 925–L927.
- [3] R.K. Willardson, A.C. Beer, *Semiconductor and Semimetals*, Academic Press, Boston, 1990.
- [4] M.Y. Shiue, Y.C. Sun, M.H. Yang, Determination of tellurium in indium antimonide semiconductor material by electrothermal atomic absorption spectrometry, *Analyst* 126 (2001) 1449–1452.
- [5] T. Fulop, C. Bekele, U. Landau, J. Angus, K. Kash, Electrodeposition of polycrystalline InSb from aqueous electrolytes, *Thin Solid Films* 449 (2004) 1–5.
- [6] Y. Sun, S.F. Cheng, G. Chen, R.F. Hicks, The effect of antimony in the growth of indium arsenide quantum dots in gallium arsenide, *J. Appl. Phys.* 97 (2005), 053503-1-6.
- [7] Jae Hun Seol, Arden L. Moore, Sanjoy K. Saha, Feng Zhou, Li Shi, Measurement and analysis of thermopower and electrical conductivity of an indium antimonide nanowire from a vapor–liquid–solid method, *J. Appl. Phys.* 101 (2007), 023706-1-6.
- [8] S. Sriram, R. Chandiramouli, DFT studies on the stability of linear, ring, and 3D structures in CdTe nanoclusters, *Res. Chem. Intermed.* (2013), <http://dx.doi.org/10.1007/s11164-013-1334-6>.
- [9] M. Valiev, E.J. Bylaska, N. Govind, K. Kowalski, T.P. Straatsma, H.J.J. Van Dam, D. Wang, J. Nieplocha, E. Apra, T.L. Windus, W.A. deJong, NWChem: a comprehensive and scalable open-source solution for large scale molecular simulations, *Comput. Phys. Commun.* 181 (2010) 1477–1489.
- [10] Refat Mahfouz, Eida Al-Frag, H. Rafiq, M. Siddiqui, Z. Waed, Al-kiali, O. Karama, New aqua rhenium oxocomplex; synthesis, characterization, thermal studies, DFT calculations and catalytic oxidations, *Arab. J. Chem.* 4 (2011) 119–124.
- [11] A. Droghetti, D. Alfè, S. Sanvito, Assessment of density functional theory for iron(II) molecules across the spin-crossover transition, *J. Chem. Phys.* 137 (2012) 124303–124312.
- [12] Mohammed Bouklah, Houria Harek, Rachid Touzani, Belkheir Hammouti, Yahia Harek, DFT and quantum chemical investigation of molecular properties of substituted pyrrolidinones, *Arab. J. Chem.* 5 (2012) 163–166.
- [13] S. Groenewold Gary, K. Gianotto Anita, E. McIlwain Michael, J. Van Stipdonk Michael, Kullman Michael, T. Moore David, Polfer Nick, Oomens Jos, Infante Ivan, Visscher Lucas, Siboulet Bertrand, A. de Jong Wibe, Infrared spectroscopy of discrete uranyl anion complexes, *J. Phys. Chem.* 112 A (2008) 508–521.
- [14] R. Chandiramouli, A DFT study on the structural and electronic properties of Barium Sulfide nanoclusters, *Res. J. Chem. Environ.* 17 (2013) 64–73.
- [15] R. Srinivasaraghavan, R. Chandiramouli, B.G. Jeyaprakash, S. Seshadri, Quantum chemical studies on CdO nanoclusters stability, *Spectrochim. Acta Part A Mol. Biomol. Spectrosc.* 102 (2013) 242–249.
- [16] M. Arivazhagan, S. Jeyavijayan, Vibrational spectroscopic, first-order hyperpolarizability and HOMO, LUMO studies of 1,2-dichloro-4-nitrobenzene based on Hartree–Fock and DFT calculations, *Spectrochim. Acta Part A Mol. Biomol. Spectrosc.* 79 (2011) 376–383.
- [17] R. John Xavier, E. Gobinath, Experimental and theoretical spectroscopic studies, HOMO–LUMO NBO and NLMO analysis of 3,5-dibromo-2,6-dimethoxy pyridine, *Spectrochim. Acta Part A: Molec. Biomolec. Spectrosc.* 97 (2012) 215–222.
- [18] Chang-Guo Zhan, J.A. Nichols, D.A. Dixon, Ionization potential, electron affinity, electronegativity, hardness, and electron excitation energy: molecular properties from density functional theory orbital energies, *J. Phys. Chem. A* 107 (2003) 4184–4195.
- [19] S. Sriram, R. Chandiramouli, D. Balamurugan, K. Ravichandran, A. Thayumanavan, Quantum chemical studies on NiO nanoclusters, *J. Atom. Molec. Sci.* 4 (4) (2013) 336–348.
- [20] S. Sriram, R. Chandiramouli, A study on the electronic properties of GaInPAs nanostructures: a density functional theory approach, *Eur. Phys. J. Plus* 128 (116) (2013) 1–8.
- [21] S. Sriram, R. Chandiramouli, D. Balamurugan, A. Thayumanvan, A DFT study on the structural and electronic properties of ZnTe nanoclusters, *Eur. Phys. J. Appl. Phys.* 62 (2013) 30101.
- [22] D. Bandyopadhyay, Chemisorptions, effect of oxygen on the geometries, electronic and magnetic properties of small size Nin ( $n = 1–6$ ) clusters, *J. Molec. Model.* 18 (2012) 737–749.
- [23] A. Dwivedi, N. Misra, Theoretical study of transition metal oxide clusters (TMnOm) [(TM–Pd, Rh, Ru) and ( $n, m = 1, 2$ )], *J. Atom. Molec. Sci.* 3 (2012) 297–307.
- [24] N. Misra, A. Dwivedi, A.K. Pandey, Structural, vibrational and electronic properties of small group IV oxide clusters in lower and higher spin state: a DFT study, *J. Atom. Molec. Sci.* 3 (2012) 187–196.
- [25] R. Chandiramouli, S. Sriram, D. Balamurugan, Quantum chemical studies on  $(\text{ZnO})_n/(\text{NiO})_n$  heterostructured nanoclusters, *Mol. Phys.* 112 (2013) 151–164.